

# A specific affinity cyclic peptide enhances the adhesion, expansion and proliferation of rat bone mesenchymal stem cells on $\beta$ -tricalcium phosphate scaffolds

TIANTONG SUN<sup>1,2</sup>, ZHENTAO MAN<sup>1</sup>, CHANGLIANG PENG<sup>3</sup>, GUOZONG WANG<sup>1,2</sup> and SHUI SUN<sup>1</sup>

<sup>1</sup>Department of Joint Surgery, Shandong Provincial Hospital Affiliated to Shandong University, Jinan, Shandong 250021; <sup>2</sup>College of Clinical Medicine, Shandong University, Jinan, Shandong 250012; <sup>3</sup>Department of Orthopedics, The Second Hospital of Shandong University, Jinan, Shandong 250033, P.R. China

Received January 5, 2019; Accepted May 14, 2019

DOI: 10.3892/mmr.2019.10335

**Abstract.** Osteonecrosis of the femoral head (ONFH) is a common osteological disease. Treatment of ONFH prior to the collapse of the femoral head is critical for increasing therapeutic efficiency. Tissue engineering therapy using bone mesenchymal stem cells (BMSCs) combined with a scaffold is a promising strategy. However, it is currently unclear how to improve the efficiency of BMSC recruitment under such conditions. In the present study, a specific cyclic peptide for Sprague-Dawley rat BMSCs, CTTNPFSLC (known as C7), was used, which was identified via phage display technology. Its high affinity for BMSCs was demonstrated using flow cytometry and fluorescence staining. Subsequently, the cyclic peptide was placed on  $\beta$ -tricalcium phosphate ( $\beta$ -TCP) scaffolds using absorption and freeze-drying processes. Adhesion, expansion and proliferation of BMSCs was investigated *in vitro* on the C7-treated  $\beta$ -TCP scaffolds and compared with pure  $\beta$ -TCP scaffolds. The results revealed that C7 had a promoting effect on the adhesion, expansion and proliferation of BMSCs on  $\beta$ -TCP scaffolds. Therefore, C7 may be effective in future tissue engineering therapy for ONFH.

## Introduction

Osteonecrosis of the femoral head (ONFH) is a debilitating skeletal disorder that occurs in young individuals. Up to 20,000 patients are diagnosed with ONFH in the United States annually (1,2). In China, it is estimated that the total number

of patients with ONFH is 5-7.5 million with 10,000-20,000 new cases each year (3). However, the pathogenesis of ONFH remains unclear, and effective preventive treatment strategies are urgently required. Once diagnosed, ~80% of patients typically progress to femoral head collapse within 1-5 years if it is not treated in a timely manner, and total hip arthroplasty (THA) is often required (4). However, limitations in the field of material science mean that, artificial hip joints are still associated with a limited service life and serious complications (5). Therefore, it is vital to identify methods to prevent the collapse of the femoral head and delay the occurrence of THA in the early stages, as well as develop effective treatment methods for ONFH (6). Core decompression combined with bone mesenchymal stem cell (BMSC)-based therapy was recently revealed to be a promising method to treat the early stages of ONFH (7-12).

BMSCs are multipotent stem cells that have the ability to self-renew and differentiate into osteoblasts, chondrocytes and adipocytes to reproduce skeletal tissues. In addition, BMSCs are associated with various technical advantages, including easy collection, rapid expansion and low immunogenicity (13,14). Thus, BMSCs have become an optimal seed cell choice in bone tissue engineering. Tissue engineering technology primarily uses exogenous/endogenous seed cells, biomaterial scaffolds with good biocompatibility and degradability, and biologically active molecules for reconstruction of defective tissues or organs (15). A number of studies suggested that BMSC-based tissue engineering has specific effects on cartilage repair and bone regeneration (16-19). For instance, a dually optimized silk-fibroin-gelatin scaffold combined with endogenous BMSC could repair cartilage injury *in vitro* and *in vivo* (16). Another study demonstrated that gene-transfected MSCs seeded on  $\beta$ -tricalcium phosphate ( $\beta$ -TCP) ceramic scaffolds promoted bone regeneration, suggesting this may be a potential strategy for the treatment of ONFH (17). Unfortunately, the low usage efficiency of exogenous BMSCs due to their poor adhesion on biomaterial scaffolds is a complication in BMSC-based tissue engineering (18,20,21). Bioactive molecules, particularly polypeptides, have been used to modify biomaterial scaffolds (19,22-24). Compared with linear peptides which these studies have focused on (19,22-24), cyclic peptides have

---

*Correspondence to:* Professor Shui Sun, Department of Joint Surgery, Shandong Provincial Hospital Affiliated to Shandong University, 324 Jingwuweiqi Road, Huaiyin, Jinan, Shandong 250021, P.R. China  
E-mail: sunshuisph@163.com

**Key words:** cyclic peptide, phage display, bone marrow mesenchymal stem cell, osteonecrosis of the femoral head,  $\beta$ -tricalcium phosphate scaffolds

several favorable properties including high affinity, selectivity and stability to protein targets (25). Phage display technology has been widely used to screen small peptides with high affinity and specificity for targets of interest, including small molecules, cells, tissues and materials, through biopanning procedures (26-28).

Previous studies have proven the success of using BMSCs combined with various biomaterial scaffolds in bone regeneration (29,30). The  $\beta$ -TCP scaffold is a bone tissue engineering material that has been widely used in the clinic for decades. The  $\beta$ -TCP scaffolds have the advantages of biocompatibility and biodegradability, and favorable osteogenesis and angiogenesis properties (31-33). Several studies have demonstrated that using  $\beta$ -TCP scaffolds combined with BMSCs could promote bone regeneration *in vitro* and *in vivo* (18,34-36). The porous structure of  $\beta$ -TCP provides a scaffold for the adhesion and growth of BMSCs while the connection between pores facilitates the blood supply of the scaffolds. However, the adhesion of BMSCs on  $\beta$ -TCP scaffolds is considered unsatisfactory, reducing the effectiveness of this promising method (18,21,37). Recently, studies have demonstrated that the implantation of  $\beta$ -TCP bioceramic scaffolds can treat early stage ONFH effectively (31,38,39). However, up to date, no research has focused on the use of cyclic peptides to improve the adhesion of BMSCs on  $\beta$ -TCP scaffolds in the tissue engineering treatments for ONFH.

In the present study,  $\beta$ -TCP scaffolds were covered with bioactive cyclic peptides in order to improve the biofunction of  $\beta$ -TCP scaffolds in tissue engineering *in vitro*. A specific affinity cyclic peptide for rat BMSCs was screened from the cyclic peptide phage display library (Ph.D.<sup>TM</sup>-C7C) using phage display technology. The affinity of the cyclic peptide for BMSCs was detected by fluorescence staining and flow cytometry. Furthermore, the cyclic peptides were also placed over the surface of the  $\beta$ -TCP scaffolds in order to investigate their effect on the adhesion, expansion and proliferation of BMSCs.

## Materials and methods

**BMSC culture.** Sprague-Dawley rat BMSCs were purchased from Cyagen Biosciences, Inc. (cat. no. RASM-X-01001). Cells were cultured in low glucose Dulbecco's modified Eagle's medium (DMEM; cat. no. 01-051-1A; Biological Industries, Ltd.) with 10% fetal bovine serum (cat. no. 04-400-1A; Biological Industries, Ltd.) and 1% penicillin-streptomycin at 37°C in a 5% CO<sub>2</sub> incubator. The trilineage-induced differentiation capacity of rat BMSCs was confirmed following a previously described method (22). Briefly, passage 2 BMSCs were induced with osteogenic, adipogenic and chondrogenic differentiation medium obtained from Cyagen Biosciences, Inc. (cat. nos. RASM-X-90021, 90031 and 90041) according to the manufacturer's instructions. After two weeks of culture, BMSCs were fixed with 4% neutral formaldehyde for 30 min. The cells for osteogenesis were stained with Alizarin red staining solution for 5 min and the cells for adipogenesis were stained with Oil Red O staining solution for 30 min, both at room temperature. The cells for chondrogenesis were fixed with 4% neutral formaldehyde for 30 min after three weeks of culture and were stained with Alcian Blue staining solution for

30 min at room temperature. Rat BMSCs of passages 3-6 were used in subsequent experiments.

**Biopanning of cyclic peptides by phage display.** Based on the different binding affinity abilities of the cyclic peptide in a loop-constrained heptapeptide (Ph.D.<sup>TM</sup>-C7C) phage display library and the target cell, the peptide that specifically bound to the BMSCs was selected through biopanning of the phage display technology. The biopanning procedure was performed following a previous described method with modifications (23,40).

The cyclic peptide phage display library used in the biopanning experiment was constructed using a Ph.D.<sup>TM</sup>-C7C Phage Display Peptide Library kit (cat. no. E8120S; New England BioLabs, Inc.). The Ph.D.<sup>TM</sup>-C7C library has complexity on the order of 10<sup>9</sup> independent clones. A pair of bilateral cysteine residues of the randomized 7 amino acids were oxidized to form a disulfide linkage, presenting the peptides to the cells as loops. BMSCs were cultured in 6 mm petri dishes and were washed twice with PBS (cat. no. 02-024-1A; Biological Industries, Ltd.) before blocking with DMEM supplemented with 5 mg/ml bovine serum albumin (BSA; cat. no. B2064-10G; Sigma-Aldrich; Merck KGaA) at 37°C in an atmosphere containing 5% CO<sub>2</sub> for 1 h. Cells were then washed six times with Tris-buffered saline with Tween 20 (TBST; 50 mM Tris-HCl pH 7.5, 150 mM NaCl +0.1% Tween-20) 6 times. Following this, the BMSCs were incubated with the Ph.D.<sup>TM</sup>-C7C phage display library [1x10<sup>11</sup> phage forming units (PFU)] for 1 h to allow the peptides to bind to the cells. Subsequently, the unbound phage clones were discarded and the poorly bound peptides were removed by washing BMSCs 10 times with TBST. The bound phages were eluted with 1 ml of 0.2 M glycine-HCl (pH 2.2; Sigma-Aldrich; Merck KGaA) combined with 1 mg/ml of BSA for 10 min. The elutions were neutralized with 150  $\mu$ l of 1 M Tris-HCl (pH 9.1). The eluted phage clones that had bound to the BMSCs were then amplified in *Escherichia coli* ER2738 (provided in the Ph.D.<sup>TM</sup>-C7C kit; cat. no. E8120S; New England BioLabs, Inc.). Subsequently, titration and purification of the bound phage clones were performed according to the manufacturer's protocol. In total, three rounds of biopanning were conducted to screen the BMSC-specific affinity cyclic peptides.

**Peptide sequencing and cyclic peptide synthesis.** Following two or three rounds of biopanning, the phage clones were selected randomly for sequencing. Phage DNA were sequenced by Genewiz, Inc., with Sanger sequencing. The primer used for sequencing was 5'-<sup>HO</sup>CCCTCATAGTTAGCGTAACG-3' (the -96 gIII sequencing primer was provided in the Ph.D.<sup>TM</sup>-C7C kit). Subsequently, the amino acid sequences of the presented cyclic peptides were analyzed using Chromas 2.6.6 software (Technelysium Pty Ltd.).

Through the biopanning experiment, a specific cyclic peptide in the BMSC-affinity clones was identified in the present study, which was termed C7. A scrambled version of the peptide containing the same seven amino acids between the two ends of cysteine in C7 was used as the negative control and termed S7. A fibronectin-derived peptide containing three amino acids (arginine, glycine and aspartic acid), which was confirmed to have a high affinity for BMSCs, was used as the

positive control and was termed RGD (21). All of the peptides were chemically synthesized using solid-phase peptide synthesis (Scilight Biotechnology, LLC), according to our previous study (41). The molecular weight of the synthesized C7 was determined using matrix-assisted laser desorption/ionization-time of flight mass spectrometry (JBI Scientific, LLC.) with positive mode, according to our previous study (42). The calibration matrix was  $\alpha$ -cyano-4-hydroxycinnamic acid and the instrument settings were as follows: 20,000 V accelerating voltage, 95% grid voltage, 200 nsec extraction delay time and  $\alpha$ v acquisition mass range between 600 and 2,000 kDa. An extra aminohexanoic acid was connected at the amino (N) terminus of all peptides to facilitate fluorescein-5-isothiocyanate (FITC; Scilight Biotechnology, LLC) labeling. Following FITC labeling, the peptides were stored at  $-20^{\circ}\text{C}$ . The FITC-labeled peptides were then dissolved in PBS at the concentration of 1 mg/ml prior to usage.

**Cyclic peptide affinity assay.** The cyclic peptide affinity assay was performed in accordance with previous studies with minor modifications (22,40).

BMSCs were cultured on 6-well tissue culture plates until 70–80% confluence was reached. Following this, BMSCs were cultured with 10  $\mu\text{M}$  FITC-labeled peptides for 1 h at  $37^{\circ}\text{C}$  to allow binding of the peptides to the cells and internalization. The cells were washed with PBS three times to remove non-bound peptides. Cells were then digested from the culture plate and centrifuged at  $250 \times g$  for 5 min at room temperature. Cell pellets were resuspended in PBS and subjected to flow cytometry (BD LSR Fortessa™; Becton, Dickinson and Company). The BMSC affinity properties of the cyclic peptide and two control peptides were analyzed quantitatively by flow cytometry at a wavelength of 488 nm, using FlowJo v10 (Tree Star, Inc). Furthermore, the BMSCs were cultured on 3.5 mm culture dishes (cat. no. D35-10-0-N; Cellvis) specifically for confocal laser microscopy until 70–80% confluence was reached. Cells were incubated with 10  $\mu\text{M}$  FITC-labeled peptides for 1 h at  $37^{\circ}\text{C}$  and washed three times with PBS. Following this, the cells were incubated with phalloidin (Phalloidin-iFluor 594 reagent; cat. no. ab176757; Abcam) for 45 min to display the cytoskeleton. The nuclei were counterstained with DAPI (cat. no. C0065; Beijing Solarbio Science & Technology Co., Ltd.) and the cells were examined under a confocal laser microscope (Zeiss LSM 800; Carl Zeiss Meditec AG). The cyclic peptide affinity assay was repeated at least three times.

**Bonding of cyclic peptides and  $\beta$ -TCP scaffolds.** Sterile  $\beta$ -TCP scaffolds were purchased from Shanghai Bio-lu Biomaterials Co., Ltd. Each scaffold was cylindrically shaped, with a diameter of 10 mm and a thickness of 3 mm. The porous  $\beta$ -TCP scaffolds had micropores (diameter, 500–600  $\mu\text{m}$ ; interconnection diameter, 120  $\mu\text{m}$ ). The C7, S7 and RGD peptides were bound to the scaffolds through absorption and a freeze-drying process according to a previously described method with minor modifications (42,43). The peptides were dissolved in sterile PBS to a concentration of 0.1 mg/ml. Following this, the  $\beta$ -TCP scaffolds were placed in the peptide solution and gently shaken to ensure that the peptides were fully adsorbed onto all exposed surfaces of the  $\beta$ -TCP scaffolds. The  $\beta$ -TCP

scaffolds and peptide solution were incubated at  $4^{\circ}\text{C}$  for 24 h. Subsequently, the scaffolds were washed gently with PBS to remove the non-adsorbed peptides, and dried in a freeze dryer (Alpha 1-2 LDplus; Martin Christ Gefriertrocknungsanlagen GmbH) for 1 h. After bonding with cyclic peptide, the scaffolds were stored in Eppendorf tubes at  $4^{\circ}\text{C}$  without light or moisture prior to the experiments. The peptide-bound  $\beta$ -TCP scaffolds were observed under a confocal laser microscope.

**BMSC behavior on the cyclic peptide-bound  $\beta$ -TCP scaffolds**  
**Cell adhesion.** The BMSC suspensions (100  $\mu\text{l}$ ;  $3 \times 10^5$  cells) were seeded on the C7-bound  $\beta$ -TCP scaffolds in 24-well culture plates. BMSCs were also seeded, at the same concentration as the C7-bound scaffolds, on the S7-bound and pure  $\beta$ -TCP scaffolds as the negative control and on RGD-bound scaffolds as the positive control. Following incubation for 12 and 24 h, the effluent non-adherent cells of four types of scaffolds were separately collected. Meanwhile, the scaffolds were washed with PBS three times to collect the inner non-adherent BMSCs. The total effluent cells were counted using a hemocytometer. The effluent cells of different scaffolds referred to BMSCs which were not adherent to the scaffolds. The number of effluent cells of each scaffold revealed the extent of BMSC adhesion and the recruitment capacity of BMSCs (16). The experiment was repeated at least three times.

**Cell expansion.** BMSCs were seeded on the C7-bound  $\beta$ -TCP scaffolds at a density of  $2 \times 10^4$  cells/ml. The S7-bound scaffolds and the pure  $\beta$ -TCP scaffolds were used as the negative control while the RGD-bound scaffolds were used as the positive control. Following 24 h of culture, the scaffolds were stained with phalloidin for 45 min to reveal the cytoskeleton of the cells and examined under a confocal laser microscope. The experiment was repeated at least three times.

**Cell proliferation.** To determine BMSC viability and proliferation on the different scaffolds, a Cell Counting Kit-8 (CCK-8; cat. no. CK04; Dojindo Molecular Technologies, Inc.) assay was performed according to the manufacturer's protocol. The C7-bound scaffolds, pure  $\beta$ -TCP scaffolds (negative control) and the RGD-bound scaffolds (positive control) were used. BMSCs ( $1 \times 10^4$  cells) were seeded onto the three types of peptide-bound scaffolds in 24-well culture plates. Following 1, 3, 5 and 7 days of culture, 30  $\mu\text{l}$  of CCK-8 solution was added to fresh DMEM and incubated at  $37^{\circ}\text{C}$  for 2 h. Following this, the optical density (OD) value was measured using a 96-well reader plate at 450 nm. The experiment was repeated at least three times.

**Statistical analysis.** All data were expressed as the mean  $\pm$  standard deviation, and were analyzed using one-way or two-way analysis of variance followed by Tukey's test for comparison of multiple groups. GraphPad Prism 7.0 software (GraphPad Software, Inc.) was used for data analysis.  $P < 0.05$  was considered to indicate a statistically significant difference.

## Results

**Identification of the high-affinity rat BMSC cyclic peptide.** Rat BMSCs were characterized using the trilineage-induced

Table I. Recovery efficiency of biopanning.

	Input titer (PFU)	Output titer (PFU)	Recovery efficiency	Fold increase
Round 1	1.0x10 <sup>11</sup>	5.8x10 <sup>4</sup>	5.8x10 <sup>-7</sup>	1
Round 2	1.0x10 <sup>11</sup>	3.9x10 <sup>6</sup>	3.9x10 <sup>-5</sup>	67
Round 3	1.0x10 <sup>11</sup>	1.8x10 <sup>7</sup>	1.8x10 <sup>-4</sup>	310

To identify the bone mesenchymal stem cell-affinity cyclic peptide phage clones, three rounds of biopanning were conducted. The recovery efficiency of each round was counted as the output divided by the input titer. In the third round of biopanning, the optimal recovery efficiency was achieved, which was 310-fold higher than that of the first round. PFU, phage forming units.

differentiation experiment (Fig. S1). The recovery efficiency after each round of biopanning was counted as the output titer divided by the input titer of the phage clones. The input titer of the C7C phages was 1.0x10<sup>11</sup> PFU for each round of biopanning. As presented in Table I, the optimal recovery efficiency was obtained in the third round of biopanning, which was 310-fold higher than that of the first round. The C7C phage clones in the last two rounds of biopanning were selected for sequencing. A total of 12 affinity phage clones were selected randomly in each round of sequencing. The BMSC-specific affinity cyclic peptide, CTTNPFSLC (termed C7), was subsequently identified using Sanger sequencing and Chromas analysis software (Table II and Fig. 1A). Furthermore, the C7 phage clones appeared five and six times (50%) among all of the assayed clones, in the second and third rounds of sequencing, respectively (Table II). In addition, other cyclic peptides (Table II) were also identified as candidates for BMSC-affinity peptide through the biopanning process. These results suggested high BMSC affinity of C7, which was further explored in the subsequent experiments.

**Affinity of C7 for BMSCs.** The affinity of the C7 cyclic peptide for BMSCs was further assayed. The C7 cyclic peptide was synthesized and the molecular weight of C7 was examined to be 1,006.95 kDa by mass spectrometry (Fig. 1B). A peptide with the same seven amino acids between the two ends of cysteine as C7 in a scrambled order (CTFNLPTSC) was used as the negative control (S7). A peptide containing three amino acids (arginine, glycine and aspartic acid) was used as the positive control (RGD). Following incubation with FITC-C7, FITC-S7 and FITC-RGD for 1 h, the BMSCs were examined by flow cytometry. The average fluorescence intensity was 2,913.0±311.0 for the rat BMSCs incubated with FITC-C7, 1,928.0±222.5 for the rat BMSCs incubated with FITC-RGD and 369.0±141.1 for the rat BMSCs incubated with FITC-S7 (Fig. 2A). The average fluorescence intensity of the BMSCs incubated with FITC-C7 was significantly increased compared with the FITC-S7 and FITC-RGD groups (n=3; P<0.01; Fig. 2B). In addition, strong fluorescent signals were observed in the FITC-C7 and FITC-RGD groups under confocal laser microscopy, whereas faint signals were observed in FITC-S7 treated cells (Fig. 3). These results suggested that C7 had a high affinity for the BMSCs, which was superior when compared with the positive control RGD.

**C7 cyclic peptide binding to the  $\beta$ -TCP scaffolds.** The C7, S7 and RGD peptides were bound to the  $\beta$ -TCP scaffolds for

Table II. Peptide sequences.

Round 1	Round 2	Round 3
No sequencing	CTTNPFSLC (5/12) CRLSMETVC (3/12) CQAPHKPWC (1/12) CHNSKSTTC (1/12) CPSSMRGTC (1/12) CILKKNVSC (1/12)	CTTNPFSLC (6/12) CQAPHKPWC (2/12) CRLSMETVC (1/12) CPSSMRGTC (1/12) CDLLESERC (1/12) CKMWNGSGC (1/12)

For rounds two and three of biopanning, 12 phage clones were selected randomly for the sequencing of affinity cyclic peptides. A specific cyclic peptide (CTTNPFSLC) appeared five times in round two and six times in round three, occupying 50% of all the sequenced cyclic peptides in round three.

24 h using natural absorption and the freeze-drying process. The peptide-bound  $\beta$ -TCP scaffolds were observed under a confocal laser microscope. As indicated in Fig. 4A, C7-bound  $\beta$ -TCP scaffolds exhibited homogeneous green fluorescence, indicating that the peptides were bound homogeneously on the surface of the  $\beta$ -TCP scaffolds. This result indicated the stable construction of C7-bound  $\beta$ -TCP scaffolds.

**Impact of the C7 cyclic peptide on the adhesion, expansion and proliferation of BMSCs on  $\beta$ -TCP scaffolds.** Following 12 and 24 h incubation on the four types of scaffolds, the effluent amount of BMSCs on the C7-bound scaffolds was lower compared with the S7-bound, the RGD-bound and the pure  $\beta$ -TCP scaffolds (Fig. 4B), indicating that the C7 peptide improved the cell adhesion and the recruitment capacity of BMSCs on the  $\beta$ -TCP scaffolds.

To investigate the expansion of the BMSCs, cells were seeded on C7-, S7-, RGD-bound and pure  $\beta$ -TCP scaffolds. Following 24 h of culture *in vitro*, the cells on the C7- and RGD-bound scaffolds were fully attached to the scaffolds and exhibited superior expansion morphologies when compared with the surface of the S7-bound and the pure  $\beta$ -TCP scaffolds (Fig. 4C-J). These results suggested that the C7 peptide promoted the expansion of BMSCs on the  $\beta$ -TCP scaffolds.

Next, the impact of C7 on cell proliferation was assayed. There was a significant difference in the numbers of viable BMSCs following 1, 3, 5 and 7 days of incubation among the

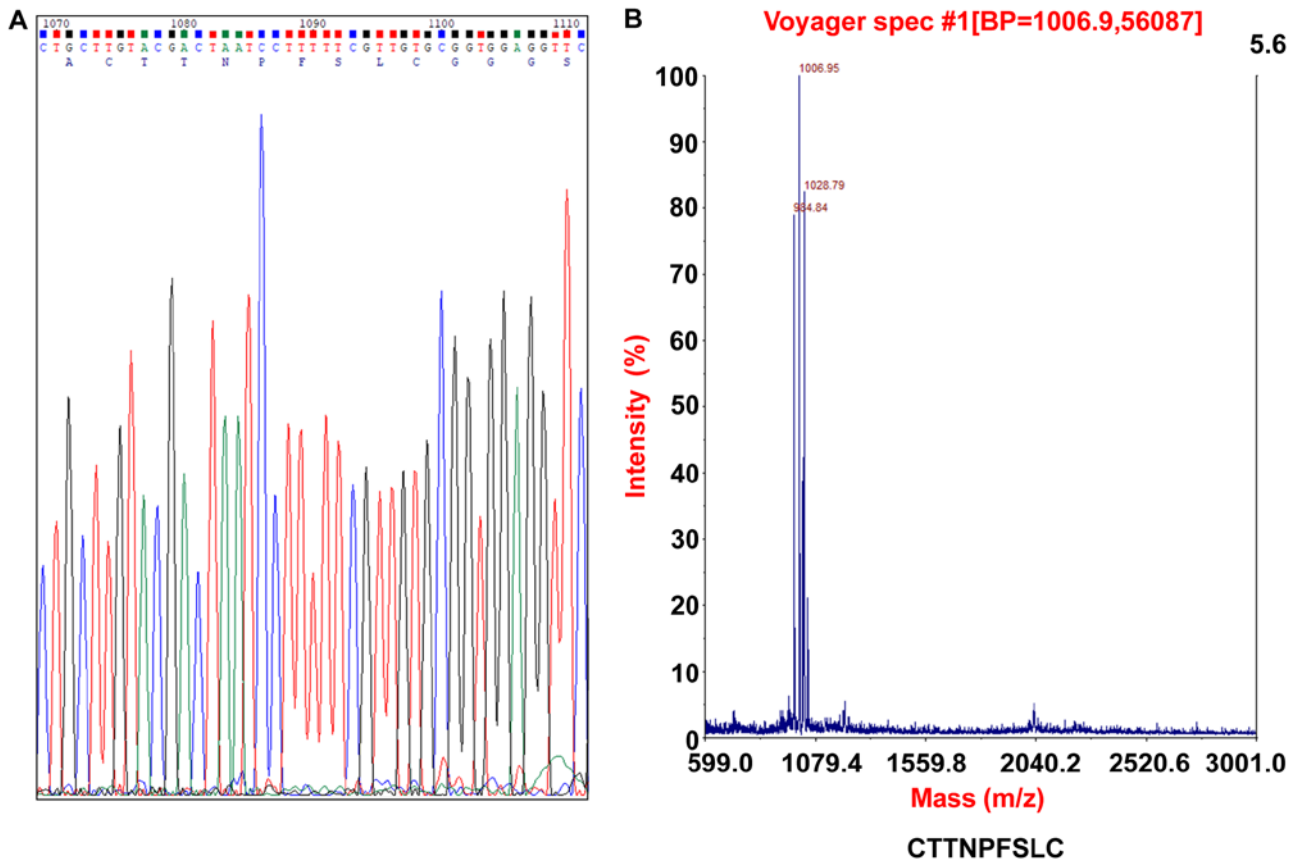


Figure 1. Identification of a cyclic peptide sequence using phage display technology. (A) The cyclic peptide sequence (CTTNPFSLC) was analyzed using Chromas software. (B) Molecular weight of cyclic peptide was determined by mass spectrometry.

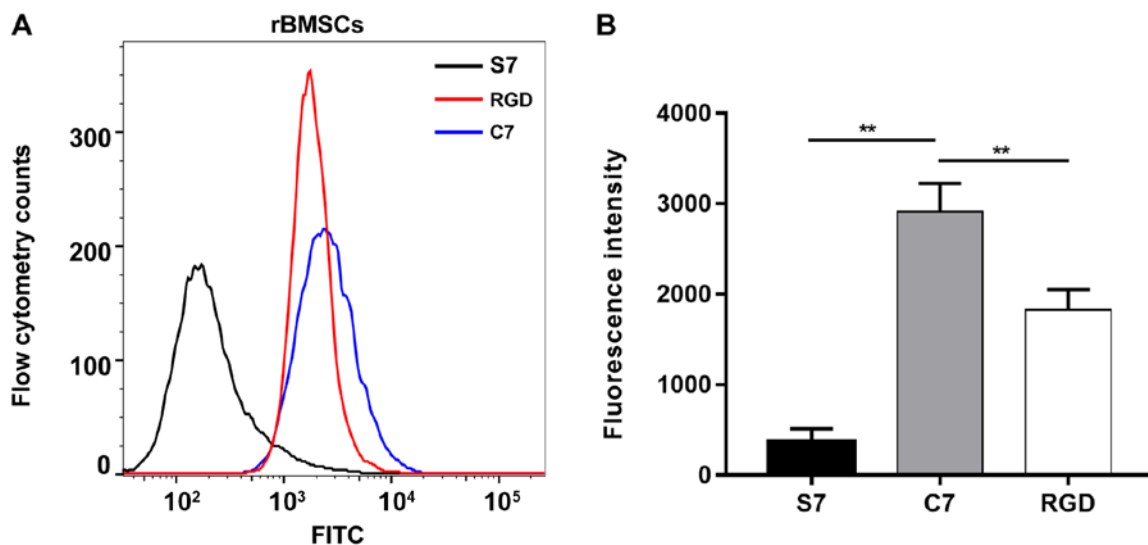


Figure 2. Affinity of the peptide for rBMSCs as determined by flow cytometry. (A) Peptide affinity was assessed following the incubation of FITC-S7, FITC-RGD and FITC-C7 with rBMSCs. Representative histograms from flow cytometry analysis are shown. (B) Average fluorescence intensity of rBMSCs incubated with different peptides (n=3). \*\*P<0.01, with comparisons indicated by lines. rBMSCs, rat bone mesenchymal stem cells; FITC, fluorescein isothiocyanate; RGD, arginine, glycine and aspartic acid.

C7- and RGD-bound, and pure  $\beta$ -TCP scaffolds. The OD value of BMSCs on C7-bound scaffolds was significantly increased compared with the pure TCP scaffolds and the RGD-bound scaffolds following 1, 3, 5 and 7 days of incubation (n=3; P<0.05; Fig. 5). Thus, it could be concluded that the C7-bound

scaffolds significantly improved the proliferation of BMSCs following a period of incubation. In addition, the OD value of BMSCs seeded on C7-bound scaffolds increased with the passage of time, demonstrating that the C7-bound scaffolds had good biocompatibility and no cytotoxicity towards BMSCs.



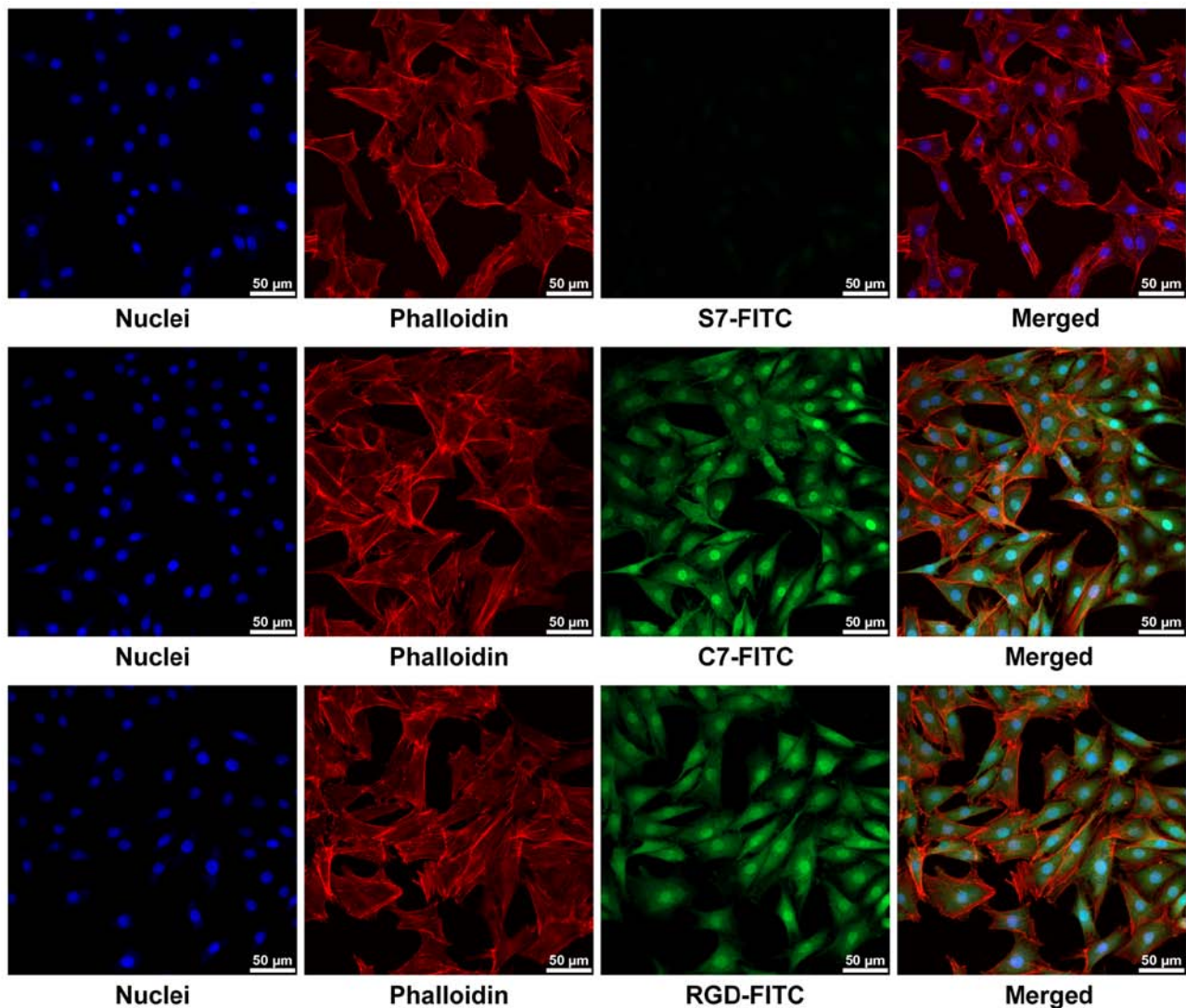


Figure 3. Affinity of the peptide for BMSCs as determined by fluorescence staining. Confocal laser microscopy images depicting peptide affinity following the incubation of BMSCs with FITC-S7, FITC-RGD, and FITC-C7 (green). The cytoskeleton was stained with phalloidin (red) and the nuclei were stained with DAPI (blue). Scale bars, 50  $\mu$ m. BMSCs, bone mesenchymal stem cells; FITC, fluorescein isothiocyanate; RGD, arginine, glycine and aspartic acid.

## Discussion

In the present study, a BMSC-specific affinity cyclic peptide (C7), which contained 7 amino acids and was disulfide cyclized, was screened using phage display technology with a Ph.D.<sup>TM</sup>-C7C phage display library. The biopanning process revealed that C7 had a specific affinity for BMSCs. Following the identification of C7, flow cytometry and fluorescent staining assays were conducted in the present study, which confirmed the high affinity of C7 for BMSCs *in vitro*. In addition,  $\beta$ -TCP scaffold surfaces were uniformly covered with C7. Subsequent experiments demonstrated improved adhesion, expansion and proliferation on C7-bound  $\beta$ -TCP scaffolds when compared with pure  $\beta$ -TCP scaffolds. In summary, the present study identified a BMSC-affinity cyclic peptide (C7) which could promote adhesion, expansion and proliferation of BMSCs on  $\beta$ -TCP scaffolds *in vitro*.

Recently, research into the bio-functionalization of bone tissue engineering materials has become a primary focus in the field of bone tissue engineering. The application of

bioactive substances can modify bone tissue engineering materials to improve their histocompatibility and biological activity. Thus, tissue engineering materials are developed from inactive materials to active materials. A common method is to modify bioactive substances, including short peptides, proteins, growth factors and other bioactive molecules, on to the surface of the materials by means of absorption or covalent coupling (44,45). Among those bioactive molecules, the biomimetic peptides are the most widely studied in the modification of bio-functionalized scaffolds due to their high purity, great bioactivity and convenient synthesis (46). Notably, our previous studies attempted to modify synthesized scaffolds with the RGD peptide and linear peptides screened by phage display technology in order to promote cell adhesion and osteogenesis (24,47). The RGD peptide is an essential cell adhesion peptide derived from fibronectin in the extracellular matrix (48). Furthermore, the RGD peptide acts as a binding ligand to the extracellular matrix protein of the targeted cells, and binds to the integrin subunit of the cell membrane. A number of biomaterials have been modified with RGD for

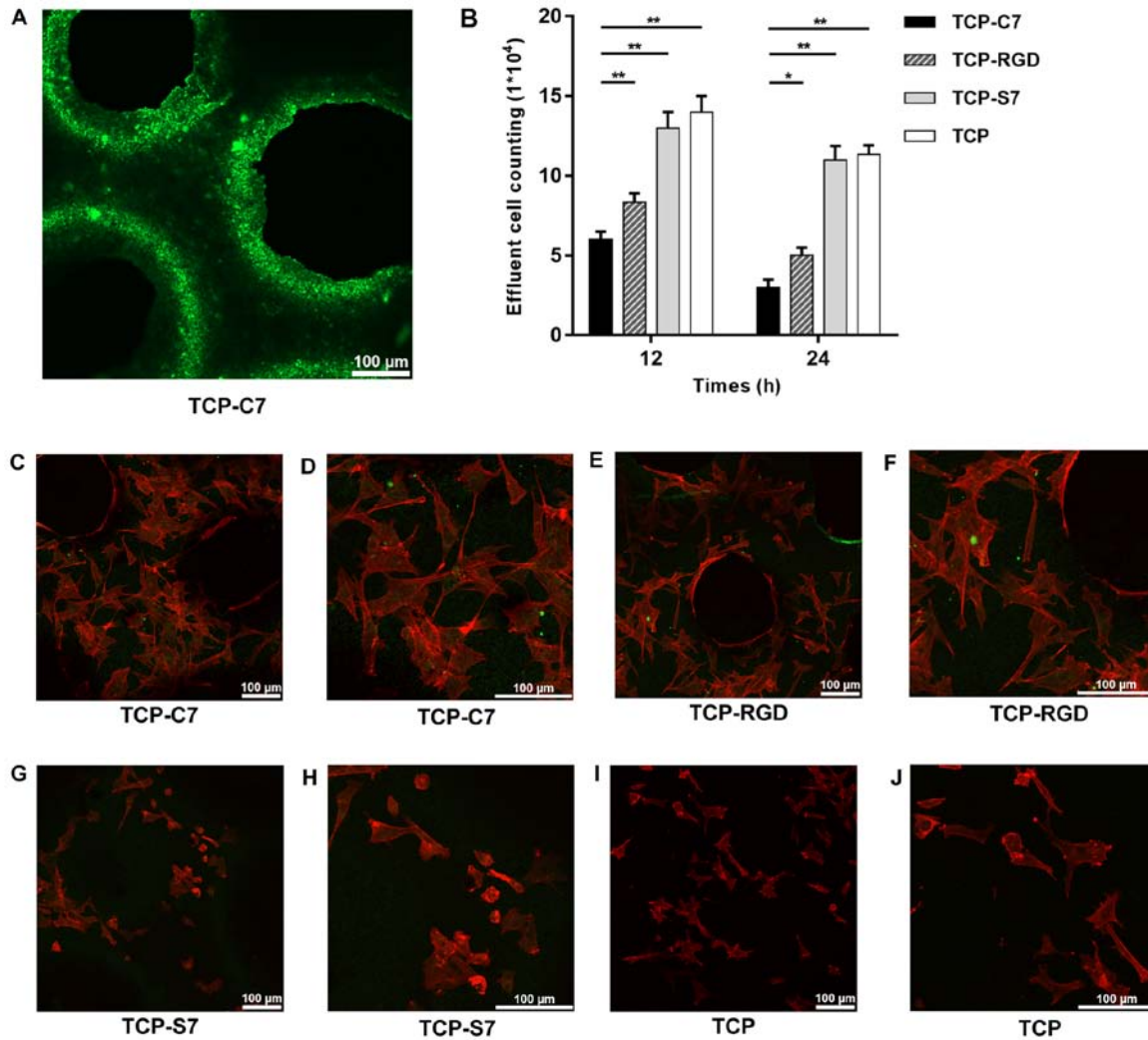


Figure 4. Adhesion and expansion of BMSCs grown on the four types of scaffold. (A) The FITC-C7 peptide was uniformly bound to the surface of  $\beta$ -TCP scaffolds. (B) Quantification of effluent cells at 12 and 24 h following BMSC seeding on the different scaffolds (n=3). \*P<0.05 and \*\*P<0.01, with comparisons indicated by lines. (C-J) Confocal laser microscopy images depicting cell expansion on the different scaffolds. Cells were visualized by staining their cytoskeleton with phalloidin (red). Following 24 h of culture *in vitro*, BMSCs grown on C7-bound and RGD-bound  $\beta$ -TCP scaffolds exhibited good expansion morphologies (C-F). By contrast, BMSCs barely expanded on S7-bound and pure  $\beta$ -TCP scaffolds (G-J). Scale bar, 100  $\mu$ m. BMSCs, bone mesenchymal stem cells; RGD, arginine, glycine and aspartic acid; TCP, tricalcium phosphate.

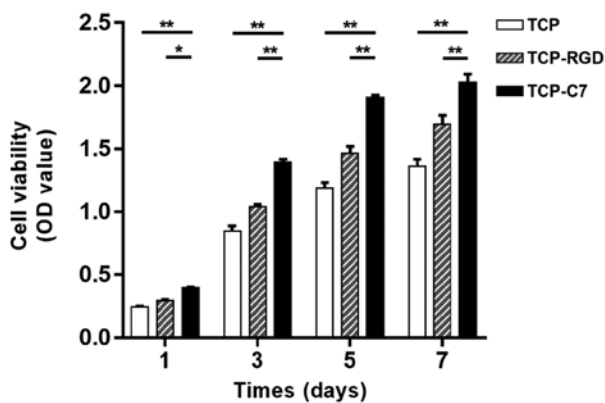


Figure 5. Proliferation of BMSCs grown on the experimental and control scaffolds. Cell proliferation was measured with the Cell Counting Kit-8 assay. Compared with BMSCs grown with the RGD-bound and pure  $\beta$ -TCP scaffolds, BMSCs on the C7-bound  $\beta$ -TCP scaffolds exhibited significantly increased proliferation following 1, 3, 5 and 7 days of incubation (n=3). \*P<0.05 and \*\*P<0.01, with comparisons indicated by lines. BMSCs, bone mesenchymal stem cells; RGD, arginine, glycine and aspartic acid; TCP, tricalcium phosphate.

medical studies and applications (49,50). However, this peptide lacks BMSC specificity due to the existence of fibronectin receptors in all cells. Recently, the utility of phage display technology has become a promising technique to search for peptides that have high BMSC affinity and specificity (22,23). According to several studies, cyclic peptides are associated with properties that make them attractive potential agents for research applications, drug development and therapeutics (25,51,52). Compared with linear peptides, cyclic peptides have higher affinity and selectivity for targets of interests, and they are more stable due to their constrained-conformation. In addition, cyclic peptides have low inherent toxicity, can be efficiently synthesized and easily labeled (25). Salmasi *et al* (53) reported that the number of seed cells, and cell adhesion and expansion on biomaterial scaffolds determined the ability of bone tissue regeneration in bone tissue engineering.

Thus, in order to improve the recruitment and the efficiency of BMSCs on biomaterial scaffolds in bone tissue engineering, the present study identified a BMSC-specific

affinity cyclic peptide, C7, using phage display technology. Using three rounds of biopanning, the recovery efficiency increased round by round. Notably, the recovery efficiency of the third round increased by 310-fold when compared with the initial round, indicating that C7 could have a specific affinity for BMSCs. The results of flow cytometry demonstrated that C7 exhibited improved BMSC affinity compared with the control S7 and RGD peptides. In addition, observation under a confocal laser microscope supported the high affinity of C7 for BMSCs. These results were similar to the affinity properties of the linear E7 peptide, which has also been identified using phage display technology (21). However, it was hypothesized that C7 may have the advantage of increased affinity due to the loop-constrained conformation with a disulfide linkage in the amino acid sequence. Following modification of the  $\beta$ -TCP scaffolds with C7 via absorption to their surface, results indicated that C7-bound  $\beta$ -TCP scaffolds exhibited superior adhesion and expansion morphologies under the confocal laser microscope when compared with pure and S7-bound  $\beta$ -TCP scaffolds, indicating that the C7-bound  $\beta$ -TCP scaffolds improved the biocompatibility of  $\beta$ -TCP scaffolds and promoted the adhesion and expansion of BMSCs. The results of effluent cell counting also supported that C7 could increase BMSC adhesion to the  $\beta$ -TCP scaffolds when compared with the other three types of scaffolds, including RGD-bound scaffolds. Thus, it could be inferred that C7 may have a superior influence on BMSC adhesion compared with the RGD peptide *in vitro*. The present study also examined the proliferation ability of BMSCs on the different scaffolds and the results were consistent with the results of cell adhesion and expansion. The OD value at 1, 3, 5 and 7 days demonstrated that C7-bound  $\beta$ -TCP scaffolds promoted the proliferation of BMSCs, compared with RGD-bound scaffolds and pure  $\beta$ -TCP scaffolds. The present results demonstrated that the cyclic peptide C7 had a specific affinity for BMSCs and improved cell adhesion, expansion and proliferation on  $\beta$ -TCP scaffolds. The present study suggested that C7 could be used to modify different biomaterials to construct bioactive scaffolds in BMSC-based tissue engineering. Future studies will need to investigate further the species specificity of C7 prior to its use in human-derived mesenchymal stem cells in clinical research in patients.

The present study has several limitations. Although C7 was isolated using phage display technology, the specificity of C7 to other subtypes of cells has not been investigated. The exact mechanism of the affinity interaction between the specific cyclic peptide and BMSCs remains unclear due to the complexities of the bioreceptors on the BMSC surface. Further studies should identify the target receptors of C7 on BMSCs and clarify how C7 activates the intracellular signaling pathway of BMSCs, thereby elucidating how the biological activities of BMSCs are regulated. In addition, further validation tests for the affinity of C7 for BMSCs in bone tissue engineering are needed. The present study lacks results from apoptosis assays to provide additional explanation of BMSCs viability on  $\beta$ -TCP. Furthermore, combined with core decompression, further investigation of C7-bound  $\beta$ -TCP scaffolds on the treatment efficacy of ONFH *in vivo* is required in the future, specifically regarding the chemotaxis

of recruiting exogenous/endogenous BMSCs and the impact on bone regeneration.

In conclusion, the present study identified a specific affinity cyclic peptide, C7, for rat BMSCs through biopanning using phage display technology. The loop-constrained heptapeptide was confirmed to be specific and have high BMSC affinity *in vitro*. In addition, in the present study, C7-bound  $\beta$ -TCP scaffolds were constructed, which exhibited improved BMSC adhesion, expansion and proliferation abilities when compared with pure  $\beta$ -TCP scaffolds *in vitro*. These results suggested that C7 could be used to enhance the recruitment of BMSCs on biomaterial scaffolds, which could provide a novel method to improve BMSC-based bone tissue engineering therapy.

### Acknowledgements

Not applicable.

### Funding

The present study was supported by the National Natural Science Foundation of China (grant no. 81702152) and the Natural Science Foundation of Shandong Province, China (grant nos. ZR2018MH007 and ZR2017BH015).

### Availability of data and materials

The datasets generated and analyzed during the current study are available from the corresponding author on reasonable request.

### Authors' contributions

TS, ZM and SS designed the experiments. TS performed the experiments. TS, CP, and GW analyzed the data. TS wrote the manuscript. TS revised the manuscript. All authors reviewed and approved the final manuscript.

### Ethics approval and consent to participate

Not applicable.

### Patient consent for publication

Not applicable.

### Competing interests

The authors declare that they have no competing interests.

### References

1. Mont MA and Hungerford DS: Non-traumatic avascular necrosis of the femoral head. *J Bone Joint Surg Am* 77: 459-474, 1995.
2. Sultan AA, Mohamed N, Samuel LT, Chughtai M, Sodhi N, Krebs VE, Stearns KL, Molloy RM and Mont MA: Classification systems of hip osteonecrosis: An updated review. *Int Orthop* 43: 1089-1095, 2019.
3. Cui L, Zhuang Q, Lin J, Jin J, Zhang K, Cao L, Lin J, Yan S, Guo W, He W, *et al.*: Multicentric epidemiologic study on six thousand three hundred and ninety five cases of femoral head osteonecrosis in China. *Int Orthop* 40: 267-276, 2016.



4. Mont MA, Cherian JJ, Sierra RJ, Jones LC and Lieberman JR: Nontraumatic osteonecrosis of the femoral head: Where do we stand today? A ten-year update. *J Bone Joint Surg Am* 97: 1604-1627, 2015.
5. Liu XW, Zi Y, Xiang LB and Wang Y: Total hip arthroplasty: a review of advances, advantages and limitations. *Int J Clin Exp Med* 8: 27-36, 2015.
6. Millikan PD, Karas V and Wellman SS: Treatment of osteonecrosis of the femoral head with vascularized bone grafting. *Curr Rev Musculoskelet Med* 8: 252-259, 2015.
7. Persiani P, De Cristo C, Graci J, Noia G, Gurzi M and Villani C: Stage-related results in treatment of hip osteonecrosis with core-decompression and autologous mesenchymal stem cells. *Acta Orthop Belg* 81: 406-412, 2015.
8. Zhao D, Cui D, Wang B, Tian F, Guo L, Yang L, Liu B and Yu X: Treatment of early stage osteonecrosis of the femoral head with autologous implantation of bone marrow-derived and cultured mesenchymal stem cells. *Bone* 50: 325-330, 2012.
9. Mao Q, Jin H, Liao F, Xiao L, Chen D and Tong P: The efficacy of targeted intraarterial delivery of concentrated autologous bone marrow containing mononuclear cells in the treatment of osteonecrosis of the femoral head: A five year follow-up study. *Bone* 57: 509-516, 2013.
10. Papakostidis C, Tosounidis TH, Jones E and Giannoudis PV: The role of 'cell therapy' in osteonecrosis of the femoral head. A systematic review of the literature and meta-analysis of 7 studies. *Acta Orthop* 87: 72-78, 2016.
11. Piuze NS, Chahla J, Schrock JB, LaPrade RF, Pascual-Garrido C, Mont MA and Muschler GF: Evidence for the Use of Cell-Based Therapy for the Treatment of Osteonecrosis of the Femoral Head: A Systematic Review of the Literature. *J Arthroplasty* 32: 1698-1708, 2017.
12. Piuze NS, Chahla J, Jiandong H, Chughtai M, LaPrade RF, Mont MA, Muschler GF and Pascual-Garrido C: Analysis of cell therapies used in clinical trials for the treatment of osteonecrosis of the femoral head: A systematic review of the literature. *J Arthroplasty* 32: 2612-2618, 2017.
13. Xie XH, Wang XL, He YX, Liu Z, Sheng H, Zhang G and Qin L: Promotion of bone repair by implantation of cryopreserved bone marrow-derived mononuclear cells in a rabbit model of steroid-associated osteonecrosis. *Arthritis Rheum* 64: 1562-1571, 2012.
14. Harada N, Watanabe Y, Sato K, Abe S, Yamanaka K, Sakai Y, Kaneko T and Matsushita T: Bone regeneration in a massive rat femur defect through endochondral ossification achieved with chondrogenically differentiated MSCs in a degradable scaffold. *Biomaterials* 35: 7800-7810, 2014.
15. Ghanaati S, Booms P, Orlowska A, Kubesch A, Lorenz J, Rutkowski J, Landes C, Sader R, Kirkpatrick C and Choukroun J: Advanced platelet-rich fibrin: A new concept for cell-based tissue engineering by means of inflammatory cells. *J Oral Implantol* 40: 679-689, 2014.
16. Shi W, Sun M, Hu X, Ren B, Cheng J, Li C, Duan X, Fu X, Zhang J, Chen H and Ao Y: Structurally and functionally optimized silk-fibroin-gelatin scaffold using 3d printing to repair cartilage injury in vitro and in vivo. *Adv Mater* 29, 2017.
17. Guo X, Zheng Q, Kulbatski I, Yuan Q, Yang S, Shao Z, Wang H, Xiao B, Pan Z and Tang S: Bone regeneration with active angiogenesis by basic fibroblast growth factor gene transfected mesenchymal stem cells seeded on porous beta-TCP ceramic scaffolds. *Biomater Mater J*: 93-99, 2006.
18. Mebarki M, Coquelin L, Layrolle P, Battaglia S, Tossou M, Hernigou P, Rouard H and Chevallier N: Enhanced human bone marrow mesenchymal stromal cell adhesion on scaffolds promotes cell survival and bone formation. *Acta Biomater* 59: 94-107, 2017.
19. Huang H, Zhang X, Hu X, Shao Z, Zhu J, Dai L, Man Z, Yuan L, Chen H, Zhou C, *et al*: A functional biphasic biomaterial homing mesenchymal stem cells for in vivo cartilage regeneration. *Biomaterials* 35: 9608-9619, 2014.
20. Diez-Escudero A, Espanol M, Bonany M, Lu X, Persson C and Ginebra MP: Heparization of beta tricalcium phosphate: Osteo-immunomodulatory effects. *Adv Healthc Mater* 7: 2018.
21. Kasten P, Lugnbuhl R, van Griensven M, Barkhausen T, Krettek C, Bohner M and Bosch U: Comparison of human bone marrow stromal cells seeded on calcium-deficient hydroxyapatite, beta-tricalcium phosphate and demineralized bone matrix. *Biomaterials* 24: 2593-2603, 2003.
22. Shao Z, Zhang X, Pi Y, Wang X, Jia Z, Zhu J, Dai L, Chen W, Yin L, Chen H, *et al*: Polycaprolactone electrospun mesh conjugated with an MSC affinity peptide for MSC homing in vivo. *Biomaterials* 33: 3375-3387, 2012.
23. Ramaraju H, Miller SJ and Kohn DH: Dual-functioning peptides discovered by phage display increase the magnitude and specificity of BMSC attachment to mineralized biomaterials. *Biomaterials* 134: 1-12, 2017.
24. Man Z, Sha D, Sun S, Li T, Li B, Yang G, Zhang L, Wu C, Jiang P, Han X, *et al*: In vitro bioactivity study of RGD-coated titanium alloy prosthesis for revision total hip arthroplasty. *Biomed Res Int* 2016: 8627978, 2016.
25. Deyle K, Kong XD and Heinis C: Phage selection of cyclic peptides for application in research and drug development. *Acc Chem Res* 50: 1866-1874, 2017.
26. Tan Y, Tian T, Liu W, Zhu Z and C JY: Advance in phage display technology for bioanalysis. *Biotechnol J* 11: 732-745, 2016.
27. Gray BP and Brown KC: Combinatorial peptide libraries: Mining for cell-binding peptides. *Chem Rev* 114: 1020-1081, 2014.
28. Zhang Y, He B, Liu K, Ning L, Luo D, Xu K, Zhu W, Wu Z, Huang J and Xu X: A novel peptide specifically binding to VEGF receptor suppresses angiogenesis in vitro and in vivo. *Signal Transduct Target Ther* 2: 17010, 2017.
29. Agarwal R and Garcia AJ: Biomaterial strategies for engineering implants for enhanced osseointegration and bone repair. *Adv Drug Deliv Rev* 94: 53-62, 2015.
30. Battiwalla M and Barrett AJ: Bone marrow mesenchymal stromal cells to treat complications following allogeneic stem cell transplantation. *Tissue Eng Part B Rev* 20: 211-217, 2014.
31. Lu Y, Lu X, Li M, Chen X, Liu Y, Feng X, Yu J, Zhang C, Niu D, Wang S, *et al*: Minimally invasive treatment for osteonecrosis of the femoral head with angioconductive bioceramic rod. *Int Orthop* 42: 1567-1573, 2018.
32. Lobo SE, Glickman R, da Silva WN, Arinze TL and Kerkis I: Response of stem cells from different origins to biphasic calcium phosphate bioceramics. *Cell Tissue Res* 361: 477-495, 2015.
33. Stulajterova R, Medvecky L, Giretova M and Sopcak T: Structural and phase characterization of bioceramics prepared from tetracalcium phosphate-monetite cement and in vitro osteoblast response. *J Mater Sci Mater Med* 26: 183, 2015.
34. Lin J, Shao J, Juan L, Yu W, Song X, Liu P, Weng W, Xu J and Mehl C: Enhancing bone regeneration by combining mesenchymal stem cell sheets with  $\beta$ -TCP/COL-I scaffolds. *J Biomed Mater Res B Appl Biomater* 106: 2037-2045, 2018.
35. Li B, Liu Z, Yang J, Yi Z, Xiao W, Liu X, Yang X, Xu W and Liao X: Preparation of bioactive  $\beta$ -tricalcium phosphate microspheres as bone graft substitute materials. *Mater Sci Eng C Mater Biol App* 70: 1200-1205, 2017.
36. Masaoka T, Yoshii T, Yuasa M, Yamada T, Taniyama T, Torigoe I, Shinomiya K, Okawa A, Morita S and Sotome S: Bone defect regeneration by a combination of a  $\beta$ -tricalcium phosphate scaffold and bone marrow stromal cells in a non-human primate model. *Open Biomed Eng J* 10: 2-11, 2016.
37. Oe K, Miwa M, Nagamune K, Sakai Y, Lee SY, Niikura T, Iwakura T, Hasegawa T, Shibamura N, Hata Y, *et al*: Nondestructive evaluation of cell numbers in bone marrow stromal cell/beta-tricalcium phosphate composites using ultrasound. *Tissue sEng Part C Methods* 16: 347-353, 2010.
38. Li B, Hu R, Sun L, Luo R, Zhao J and Tian X: A CARE-compliant article: Biomechanics of treating early-stage femoral-head osteonecrosis by using a beta-tricalcium phosphate bioceramic rod system: A 3-dimensional finite-element analysis. *Medicine (Baltimore)* 97: e10808, 2018.
39. Kawai T, Shanjan Y, Fazeli S, Behn AW, Okuzu Y, Goodman SB and Yang YP: Customized, degradable, functionally graded scaffold for potential treatment of early stage osteonecrosis of the femoral head. *J Orthop Res* 36: 1002-1011, 2018.
40. Pi Y, Zhang X, Shi J, Zhu J, Chen W, Zhang C, Gao W, Zhou C and Ao Y: Targeted delivery of non-viral vectors to cartilage in vivo using a chondrocyte-homing peptide identified by phage display. *Biomaterials* 32: 6324-6332, 2011.
41. Wang G, Man Z, Zhang N, Xin H, Li Y, Sun T and Sun S: Biopanning of mouse bone marrow mesenchymal stem cell affinity for cyclic peptides. *Mol Med Rep* 19: 407-413, 2019.
42. Wang G, Man Z, Xin H, Li Y, Wu C and Sun S: Enhanced adhesion and proliferation of bone marrow mesenchymal stem cells on betatricalcium phosphate modified by an affinity peptide. *Mol Med Rep* 19: 375-381, 2019.
43. Bhatnagar RS, Qian JJ, Wedrychowska A, Sadeghi M, Wu YM and Smith N: Design of biomimetic habitats for tissue engineering with P-15, a synthetic peptide analogue of collagen. *Tissue Eng* 5: 53-65, 1999.

44. Lutolf MP and Hubbell JA: Synthetic biomaterials as instructive extracellular microenvironments for morphogenesis in tissue engineering. *Nat Biotechnol* 23: 47-55, 2005.
45. Weber D, Kotzsch A, Nickel J, Harth S, Seher A, Mueller U, Sebald W and Mueller TD: A silent H-bond can be mutationally activated for high-affinity interaction of BMP-2 and activin type IIB receptor. *BMC Struct Biol* 7: 6, 2007.
46. Collier JH and Segura T: Evolving the use of peptides as components of biomaterials. *Biomaterials* 32: 4198-4204, 2011.
47. Man Z, Li T, Zhang L, Yuan L, Wu C, Li P, Sun S and Li W: E7 peptide-functionalized Ti6Al4V alloy for BMSC enrichment in bone tissue engineering. *Am J Transl Res* 10: 2480-2490, 2018.
48. Ruoslahti E and Pierschbacher MD: Arg-Gly-Asp: A versatile cell recognition signal. *Cell* 44: 517-518, 1986.
49. Hersel U, Dahmen C and Kessler H: RGD modified polymers: Biomaterials for stimulated cell adhesion and beyond. *Biomaterials* 24: 4385-4415, 2003.
50. Zhang H, Lin CY and Hollister SJ: The interaction between bone marrow stromal cells and RGD-modified three-dimensional porous polycaprolactone scaffolds. *Biomaterials* 30: 4063-4069, 2009.
51. Valeur E, Gueret SM, Adihou H, Gopalakrishnan R, Lemurell M, Waldmann H, Grossmann TN and Plowright AT: New modalities for challenging targets in drug discovery. *Angew Chem Int Ed Engl* 56: 10294-10323, 2017.
52. Zorzi A, Deyle K and Heinis C: Cyclic peptide therapeutics: Past, present and future. *Curr Opin Chem Biol* 38: 24-29, 2017.
53. Salmasi S, Nayyer L, Seifalian AM and Blunn GW: Nanohydroxyapatite effect on the degradation, osteoconduction and mechanical properties of polymeric bone tissue engineered scaffolds. *Open Orthop J* 10: 900-919, 2016.



This work is licensed under a Creative Commons Attribution-NonCommercial-NoDerivatives 4.0 International (CC BY-NC-ND 4.0) License.